Chapter 8
20 Years of "Noise": Contributions of Computational Neuroscience to the Exploration of the Effect of Background Activity on Central Neurons

Alain Destexhe

Abstract The central nervous system is subject to many different forms of noise, which have fascinated researchers since the beginning of electrophysiological recordings. In cerebral cortex, the largest amplitude noise source is the "synaptic noise," which is dominant in intracellular recordings in vivo. The consequences of this background activity are a classic theme of modeling studies. In the last 20 years, this field tremendously progressed as the synaptic noise was measured for the first time using quantitative methods. These measurements have allowed computational models not only to be more realistic and closer to the biological data but also to investigate the consequences of synaptic noise in more quantitative terms, measurable in experiments. As a consequence, the "high-conductance state" conferred by this intense activity in vivo could also be replicated in neurons maintained in vitro using dynamic-clamp techniques. In addition, mathematical approaches of stochastic systems provided new methods to analyze synaptic noise and obtain critical information such as the optimal conductance patterns leading to spike discharges. It is only through such a combination of different disciplines, such as experiments, computational models, and theory, that we will be able to understand how noise participates to neural computations.

Introduction

The central nervous system is subject to many different forms of noise, which have fascinated researchers since the beginning of electrophysiological recordings. In cerebral cortex, the largest amplitude noise source is the "synaptic noise,"

A. Destexhe (✉)
Unité de Neuroscience Information et Complexité (UNIC),
CNRS, Gif-sur-Yvette 91198, France
e-mail: destexhe@unic.cnrs-gif.fr

J.M. Bower (ed.), *20 Years of Computational Neuroscience*, Springer Series in Computational Neuroscience 9, DOI 10.1007/978-1-4614-1424-7_8,

which is dominant in intracellular recordings in vivo. Indeed, one of the most striking characteristics of awake and attentive states is the highly complex nature of cortical activity. Global measurements, such as the electroencephalogram (EEG) or local field potentials (LFPs), display low amplitude and very irregular activity, the so-called desynchronized EEG (Steriade 2003). This activity has very low spatiotemporal coherence between multiple sites in cortex, which contrasts with the widespread synchronization in slow-wave sleep (Destexhe et al. 1999). Local measurements, such as extracellular (unit activity) or intracellular recordings of single neurons, also demonstrate very irregular spike discharge and high levels of fluctuations similar to noise (Steriade et al. 2001), as shown in Fig. 8.1. Multiple unit activity (Fig. 8.1A) shows that the firing is irregular and of low correlation between different cells, while intracellular recordings (Fig. 8.1B) reveal that the membrane potential (V_m) is dominated by intense fluctuations ("noise").

How neurons integrate synaptic inputs in such noisy conditions is a problem which was identified in early work on motoneurons (Barrett and Crill 1974; Barrett 1975), which was followed by studies in Aplysia (Bryant and Segundo 1976) and cerebral cortex (Holmes and Woody 1989). This early work motivated further studies using compartmental models in cortex (Bernander et al. 1991) and cerebellum (Rapp et al. 1992; De Schutter and Bower 1994). These studies pointed out that the integrative properties of neurons can be drastically different in such noisy states. However, at the time, no precise experimental measurements were available to characterize the noise sources in neurons.

How neurons integrate their inputs in such states and, more generally, how entire populations of neurons represent and process information in such noisy states are still highly debated. In this chapter, we will describe recent measurements and associated progress to characterize the nature and the impact of this noisy activity. We will show that a series of major progress have been made in the last 20 years, and that computational neuroscience has played a particularly important role in this exploration.

Characterization of Synaptic Noise In Vivo

A first major advance was that this amount of "noise" was characterized and measured for the first time using quantitative methods. Figure 8.2 illustrates such measurements (Paré et al. 1998; Destexhe and Paré 1999). This first quantitative characterization was done using the "up-states" of ketaminexylazine anesthesia, which display very similar network activity as the awake brain (they were later measured in awake animals; Rudolph et al. 2007). The experiments were designed such that the same cell could be recorded before and after total suppression of network activity. A powerful blocker of network activity (tetrodotoxin, TTX) was micro-perfused during the intracellular recordings, enabling characterization of the membrane state before and after TTX infusion (Fig. 8.2, top scheme). The comparison between these two states included measuring the membrane potential (Fig. 8.2A), input resistance (Fig. 8.2B), and voltage distributions (Fig. 8.2C). These experiments

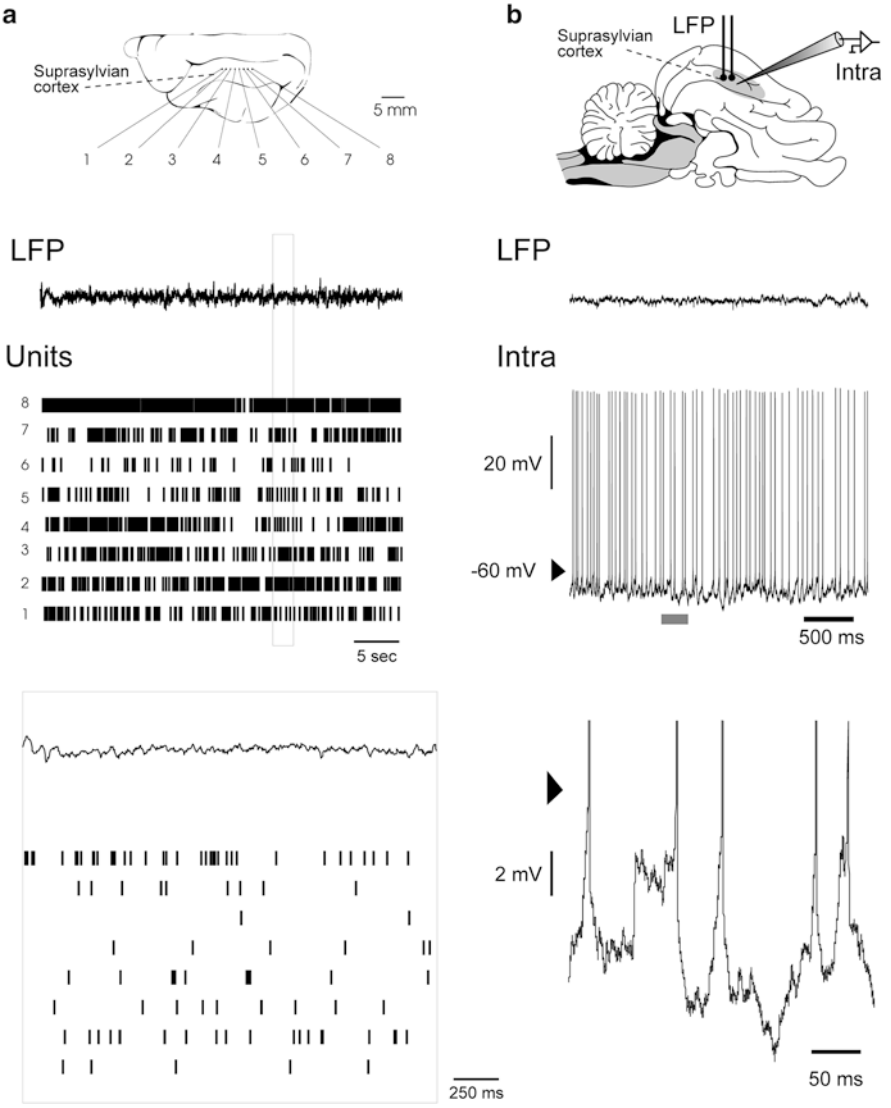

Fig. 8.1 Highly complex and "noisy" cortical activity during wakefulness. (**a**) Irregular firing activity of eight multiunits shown at the same time as the local field potential (LFP) recorded in electrode 1 (scheme on *top*). During wakefulness, the LFP is of low amplitude and irregular activity ("desynchonized") and unit activity is sustained and irregular (see magnification below; 20 times higher temporal resolution). (**b**) Intracellular activity in the same brain region during wakefulness. Spiking activity was sustained and irregular, while the membrane potential displayed intense fluctuations around a relatively depolarized state (around −65 mV in this cell; see magnification below). (**a**) Modified from Destexhe et al. 1999; (**b**) modified from Steriade et al. 2001

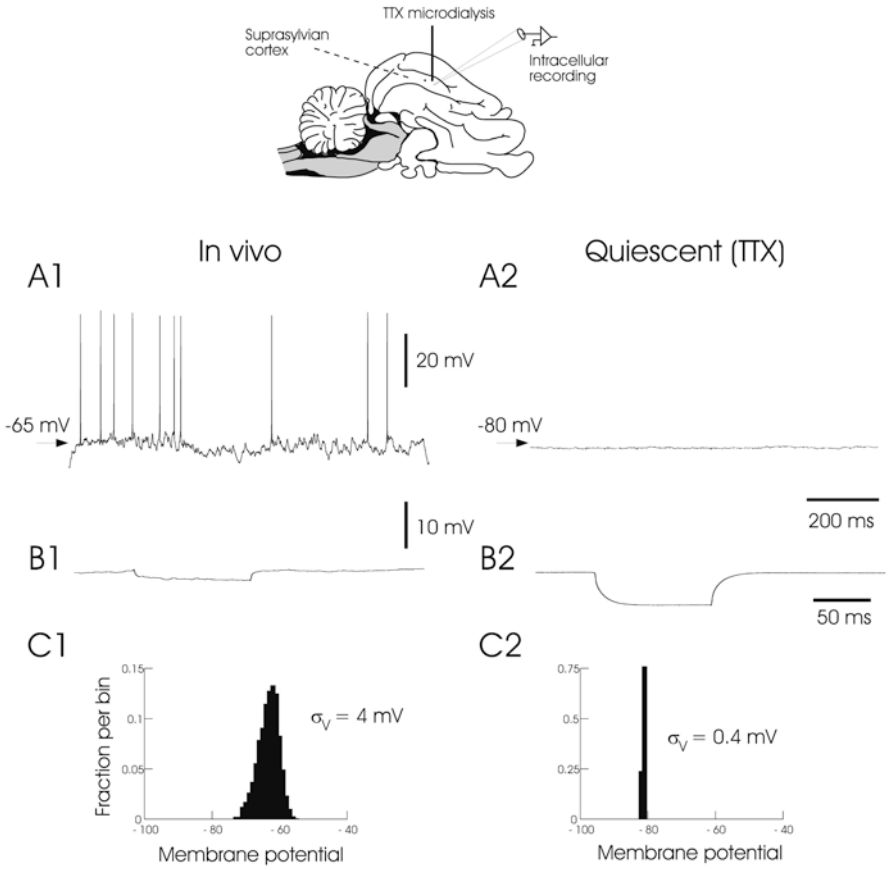

Fig. 8.2 Characterization of synaptic noise by suppression of network activity using micro-perfusion of tetrodotoxin (TTX). *Top*: experimental setup; a micro-perfusion pipette was used to infuse TTX into the cortex in vivo, at the same time of the intracellular recording. *Left*: characterization of network states in vivo. *Right*: same measurements after dialysis of TTX. The different measurements are the membrane potential (**A**), the averaged response to hyperpolarizing pulses (**B**), and the voltage distribution (**C**). (**A**–**C**) Modified from Destexhe and Paré 1999

revealed that about 80 % of the membrane conductance is attributable to synaptic activity (Paré et al. 1998; Destexhe and Paré 1999), demonstrating that neurons in vivo operate in a "high-conductance state."

Detailed Biophysical Models of Synaptic Noise

Investigating the consequences of noisy background activity is a classic theme which started by studies in motoneurons (Barrett and Crill 1974; Barrett 1975) and followed by model studies of neurons in cerebral cortex (Holmes and Woody 1989;

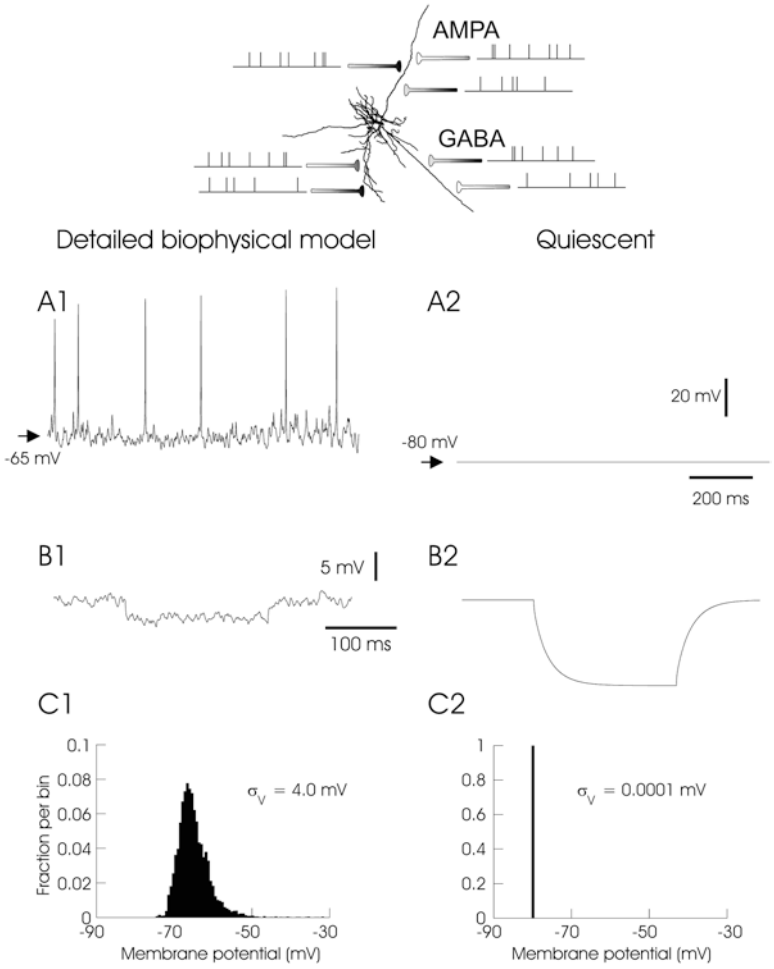

Fig. 8.3 Detailed biophysical models of synaptic background activity in cortical pyramidal neurons. *Top*: scheme of the model, based on a reconstructed cell morphology from cat parietal cortex. The model can reproduce the main features of in vivo measurements ((**A**)–(**C**) arranged similarly as Fig. 8.2). Figure modified from Destexhe et al. 2001

Bernander et al. 1991) and cerebellum (Rapp et al. 1992; De Schutter and Bower 1994). The measurements of synaptic background activity outlined above (Paré et al. 1998) have allowed computational models not only to be more realistic and closer to the biological data but also to investigate the consequences of synaptic noise in more quantitative terms. Figure 8.3 summarizes a first approach consisting of biophysically detailed models based on morphologically accurate reconstructions of cortical pyramidal neurons, combined with realistic patterns of synaptic input and intrinsic voltage-dependent conductances (see details and parameters in Destexhe and Paré 1999). These models could be tuned to reproduce all experimental measurements (Fig. 8.3A–C).

Such detailed biophysical models have been used to investigate the consequences of synaptic background activity in cortical neurons, starting with the first investigation of this kind by Bernander et al. (1991). This study revealed that the presence of background activity, although at the time nonconstrained by experimental measurements, was able to change several features of the integrative properties of the cell, such as coincidence detection.

Using models constrained from experiments, such as that of Fig. 8.3, enabled the derivation of several interesting properties, which we enumerate here.

1. *Enhanced responsiveness*. The presence of background activity was found to markedly change the cell's excitability, and produce a detectable response to inputs that are normally subthreshold (Hô and Destexhe 2000). This prediction was verified in dynamic-clamp experiments (see section "Synaptic Noise in Dynamic-Clamp").
2. *Location-independence*. The effectiveness of synaptic inputs becomes much less dependent on their position in dendrites, as found in cerebellar (De Schutter and Bower 1994) and cortical neurons (Rudolph and Destexhe 2003b), although based on very different mechanisms.
3. *Different integrative mode*. As initially predicted by Bernander et al. (1991), this important property was indeed confirmed with models constrained by experimental measurements (Rudolph and Destexhe 2003b).
4. *Enhanced temporal processing*. As a direct consequence of the "high-conductance state" of the neurons under background activity, the faster membrane time constant allows the neuron to perform finer discrimination, which is essential for coincidence detection (Softky 1994; Rudolph and Destexhe 2003b; Destexhe et al. 2003) or detecting brief changes of correlation (Rudolph and Destexhe 2001). The latter prediction was also verified experimentally (Fellous et al. 2003).
5. *Modulation of intrinsic properties*. It was found that in the presence of synaptic background activity, the responsiveness of bursting neurons is strongly affected (Wolfart et al. 2005). This aspect will be considered in more detail below.

These properties have been summarized and detailed in different review papers and books (Destexhe et al. 2003; Destexhe 2007; Haider and McCormick 2009; Destexhe and Rudolph 2012) which should be consulted for more information.

Simplified Models of Synaptic Noise

A second major step was to obtain simplified representations that capture the main properties of the synaptic "noise." This advance is important, because simple models have enabled real-time applications such as the dynamic-clamp (see section "Synaptic Noise in Dynamic-Clamp"). Simple models also have enabled a number of mathematical treatments, some of which resulted in methods to analyze experiments, as outlined in sections "Stochastic Systems Analysis of Synaptic Noise" and

"Estimating the Optimal Conductance Patterns Leading to Spikes in 'Noisy' States." These approaches relied on a simplified model of synaptic noise, called the "point-conductance model" (Destexhe et al. 2001), which can be written as:

$$C\frac{dv}{dt} = -g_{\mathrm{L}}(V - E_{\mathrm{L}}) - g_{\mathrm{e}}(V - E_{\mathrm{e}}) - g_{\mathrm{i}}(V - E_{\mathrm{i}}) + I_{\mathrm{ext}} \tag{8.1}$$

$$\frac{dg_{\mathrm{e}}(t)}{dt} = -\frac{1}{\tau_{\mathrm{e}}}\left[g_{\mathrm{e}}(t) - g_{\mathrm{e0}}\right] + \sqrt{\frac{2\sigma_{\mathrm{e}}^2}{\tau_{\mathrm{e}}}}\xi_{\mathrm{e}}(t) \tag{8.2}$$

$$\frac{dg_{\mathrm{i}}(t)}{dt} = -\frac{1}{\tau_{\mathrm{i}}}\left[g_{\mathrm{e}}(t) - g_{\mathrm{i0}}\right] + \sqrt{\frac{2\sigma_{\mathrm{i}}^2}{\tau_{\mathrm{i}}}}\xi_{\mathrm{i}}(t) \tag{8.3}$$

where C denotes the membrane capacitance, I_{ext} a stimulation current, g_{L} the leak conductance, and E_{L} the leak reversal potential. $g_{\mathrm{e}}(t)$ and $g_{\mathrm{i}}(t)$ are stochastic excitatory and inhibitory conductances with respective reversal potentials E_{e} and E_{i}. The excitatory synaptic conductance is described by Ornstein–Uhlenbeck (OU) stochastic processes (8.2), where g_{e0} and σ_{e}^2 are, respectively, the mean value and variance of the excitatory conductance, τ_{e} is the excitatory time constant, and $\xi_{\mathrm{e}}(t)$ is a Gaussian white noise source with zero mean and unit standard deviation. The inhibitory conductance $g_{\mathrm{i}}(t)$ is described by an equivalent equation (8.3) with parameters g_{i0}, σ_{i}^2, τ_{i}, and noise source $\xi_{\mathrm{i}}(t)$. Note that all conductances are here expressed in absolute units (in nS) but a formulation in terms of conductance densities is also possible.

In many previous models, synaptic activity was modeled by a source of current noise in the neuron (Tuckwell 1988), and thus the membrane potential is equivalent to a stochastic process. In contrast, in the point-conductance model, the conductances are the stochastic processes, and the V_{m} fluctuations result from the combined action of two of such fluctuating conductances. This model is thus capable of reproducing all features of the high-conductance state found in cortical neurons in vivo, such as large-amplitude fluctuations, low input resistance, and depolarized V_{m} (Fig. 8.4). In addition, it also captures the correct power spectral structure of the synaptic conductances (see Destexhe et al. 2001).

Synaptic Noise in Dynamic-Clamp

An elegant technique to investigate the effect of synaptic noise on neurons is to use the dynamic-clamp technique (Robinson and Kawai 1993; Sharp et al. 1993; for a recent review, see Destexhe and Bal 2009). This technique can be used to artificially reproduce stochastic synaptic activity by injecting the corresponding computer-generated conductance in a living neuron (Destexhe et al. 2001; Chance et al. 2002;

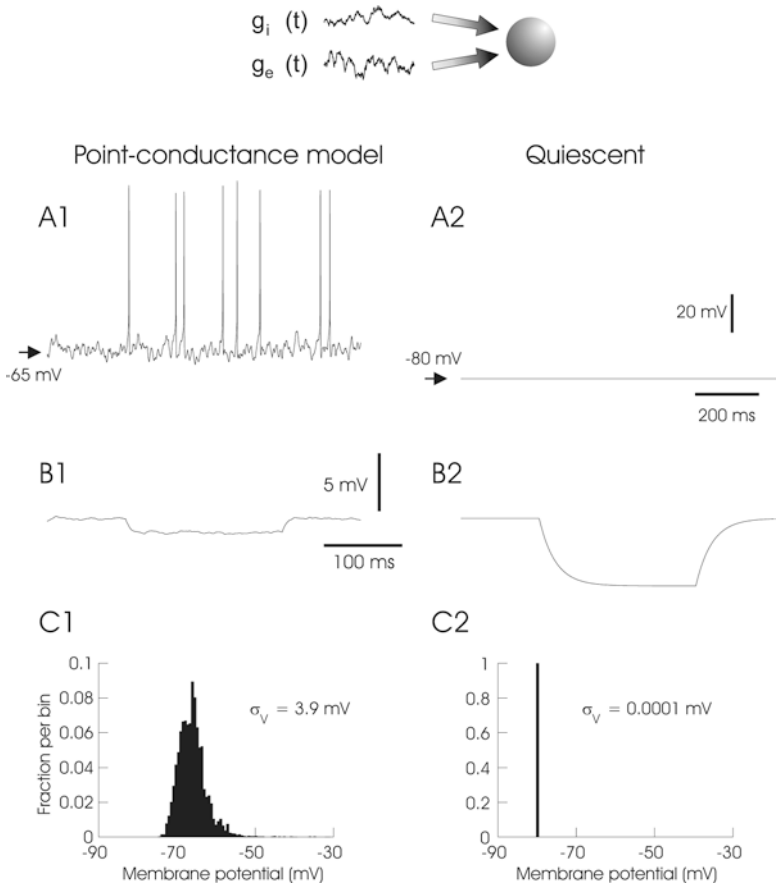

Fig. 8.4 Point-conductance model of synaptic background activity in cortical neurons. *Top*: scheme of the point-conductance model, where two stochastically varying conductances determine the V_m fluctuations through their (multiplicative) interaction. This simplified model reproduces the main features of in vivo measurements (same arrangement of (**A**)–(**C**) as in Fig. 8.2). Figure modified from Destexhe et al. 2001

Fellous et al. 2003; Mitchell and Silver 2003; Prescott and De Koninck 2003; Shu et al. 2003). This approach was first applied to cortical neurons, and revealed an important effect of the stochastic synaptic activity on neuronal responsiveness (Destexhe et al. 2001; Chance et al. 2002; Mitchell and Silver 2003; Prescott and De Koninck 2003; Shu et al. 2003; Higgs et al. 2006), similar to computational model predictions (Hô and Destexhe 2000). Some of these properties are reminiscent of the "stochastic resonance" phenomenon, which is an optimal signal-to-noise ratio in nonlinear systems subject to noise, and which was long studied by physicists (Wiesenfeld and Moss 1995; Gammaitoni et al. 1998).

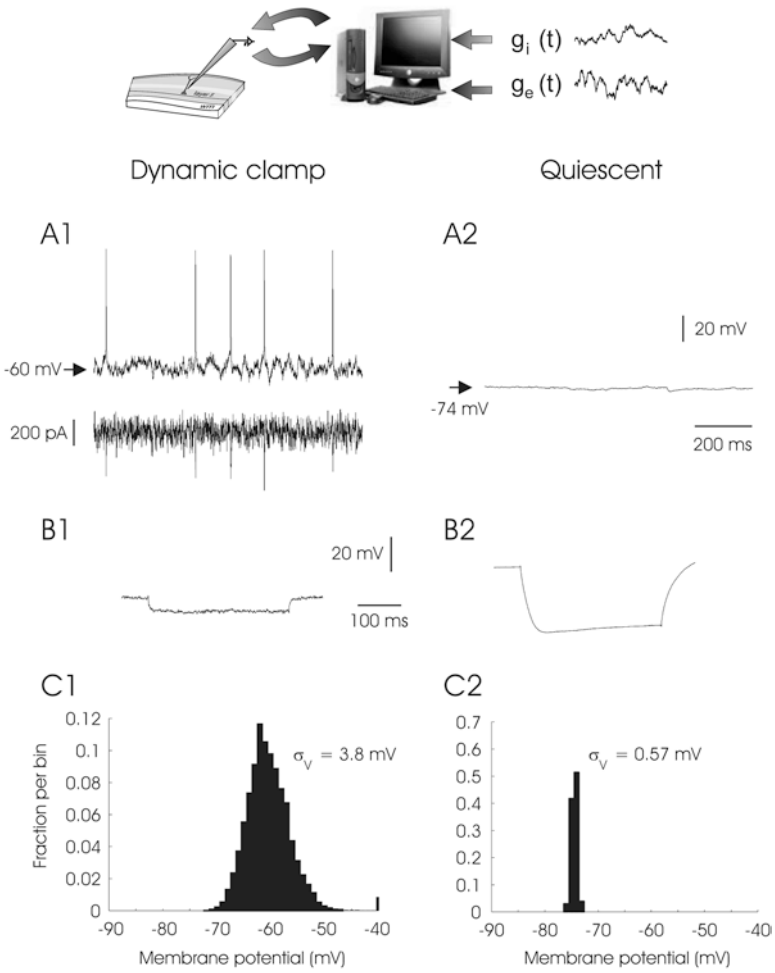

Fig. 8.5 Dynamic-clamp recreation of high-conductance states in neurons in vitro. *Top*: scheme of the dynamic-clamp, the point-conductance model is simulated and the excitatory and inhibitory conductances are injected in a living neuron using dynamic-clamp. This technique enables obtaining states very similar to in vivo measurements (similar arrangement of panels as Fig. 8.2). Figure modified from Destexhe et al. 2001

Figure 8.5 shows the "high-conductance state" conferred by intense synaptic activity, as replicated in neurons maintained in vitro using the dynamic-clamp technique. As for models, this technique enables the experimentalist to reproduce (and modulate at will) a background activity with similar properties as found in vivo.

Perhaps the most unexpected property of synaptic noise was found when investigating the effect of noise on thalamic neurons (Wolfart et al. 2005). These neurons are classically known to display two distinct firing modes, a single-spike (tonic) mode and a burst mode at more hyperpolarized levels (Llinas and Jahnsen 1982).

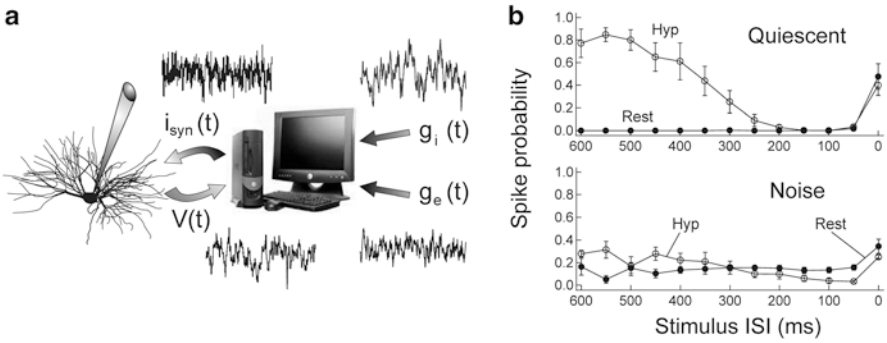

Fig. 8.6 Dynamic-clamp investigation of the transfer function of thalamic neurons in vitro. (**a**) Scheme of the dynamic-clamp experiment, in which stochastic conductances are injected in the neuron. (**b**) Effect of synaptic noise in thalamic neurons. The conductance noise interacts with burst generation to generate transfer response curves that are roughly independent on the V_m. (**b**) Modified from Wolfart et al. 2005

However, thalamic neurons are also known to receive large amounts of synaptic noise through their numerous direct synaptic connections from descending cortico-thalamic fibers, and this activity accounts for about half of the input resistance of thalamic neurons (Contreras et al. 1996). Based on these measurements, the effect of synaptic noise was simulated using dynamic-clamp on thalamic neurons in slices, and remarkably it was found that under such in vivo-like conditions, the duality of firing modes disappears because single spikes and bursts now appear at all V_m levels (Wolfart et al. 2005). But more interestingly, if one calculates the full transfer function of the neuron, the amount of spikes transmitted to cortex becomes independent of the V_m level (Fig. 8.6). This property is due to the fact that for hyperpolarized V_m, the low-threshold Ca^{2+} current generates more bursts, and thus "compensates" for hyperpolarization. This remarkable property shows that both the intrinsic properties and synaptic noise are necessary to understand the transfer function of central neurons in vivo.

Stochastic Systems Analysis of Synaptic Noise

Another consequence of the simplicity of the point-conductance model is that it enables mathematical approaches. In particular, if one could obtain an analytic expression of the steady-state voltage distribution (such that shown in Fig. 8.2C1), fitting such an expression to experimental data could yield estimates of conductances and other parameters of background activity. This idea was formulated for the first time less than 10 years ago (Rudolph and Destexhe 2003a) and subsequently gave rise to a method called the "VmD method" (Rudolph et al. 2004), which we outline here.

The method to obtain an analytical expression for the voltage distribution is to consider the point-conductance model ((8.1), (8.2), and (8.3)) and evaluate the probability density of finding the system at a value V at time t, denoted $\rho(V, t)$. The time evolution of this probability density is given by a Fokker–Planck equation (Risken 1984), and at steady-state, the probability density gives the voltage distribution $\rho(V)$. So obtaining an analytic estimate of this voltage distribution requires finding the steady-state solution of the Fokker–Planck equation for the system ((8.1), (8.2), and (8.3)). However, this system is nonlinear due to the presence of conductances and their multiplicative effect on the membrane potential, so the corresponding Fokker–Planck equation is not solvable, and one has to rely on approximations. This problem was studied by several groups who proposed different approximations to this problem (Rudolph and Destexhe 2003a, 2005; Richardson 2004; Lindner and Longtin 2006; for a comparative study, see Rudolph and Destexhe 2006).

One of these expressions is invertible (Rudolph and Destexhe 2003a, 2005), which enables one to directly estimate the parameters (g_{e0}, g_{i0}, σ_e, σ_i) from experimentally calculated V_m distributions. This constitutes the basis of the VmD method (Rudolph et al. 2004).

One main assumption behind this method is that the conductance variations are Gaussian-distributed, and thus this distribution can be described by the mean (g_{e0}, g_{i0}) and the standard deviations (σ_e, σ_i) for each conductance. We use the following expression for V_m fluctuations

$$\rho(V) \sim \exp\left[-\frac{(V-\bar{V})^2}{2\sigma_V^2}\right]$$

where $\bar{V}$ is the average V_m and σ_V its standard deviation. This expression provides an excellent approximation of the V_m distributions obtained from models and experiments (Rudolph et al. 2004), because the V_m distributions obtained experimentally show little asymmetry (for up-states and activated states; for specific examples, see Rudolph et al. 2004, 2005, 2007).

This Gaussian distribution can be inverted, which leads to expressions of the synaptic noise parameters as a function of the V_m measurements, $\bar{V}$ and σ_V. To extract the four parameters, means (g_{e0}, g_{i0}) and standard deviations (σ_e, σ_i), from the V_m requires to measure two V_m distributions obtained at two different constant levels of injected current. In this case, the Gaussian fit of the two distributions gives two mean V_m values, $\bar{V}_1$ and $\bar{V}_2$, and two standard deviation values, σ_{V_1} and σ_{V_2}. The system can be solved for four unknowns, leading to expressions of g_{e0}, g_{i0}, σ_e, σ_i from the values of $\bar{V}_1$, $\bar{V}_2$, σ_{V_1}, and σ_{V_2} (for details, see Rudolph et al. 2004).

This method was tested using controlled conductance injection in neurons using the dynamic-clamp technique, as shown in Fig. 8.7. In this experiment, cortical neurons were recorded in slices displaying spontaneous "up-states" of activity. These up-states were analyzed by computing their V_m distribution, which was then used to evaluate the synaptic conductance parameters according to the VmD method. This estimate of conductances was then used to generate synthetic conductance noise traces, which were injected in the same neuron during silent states.

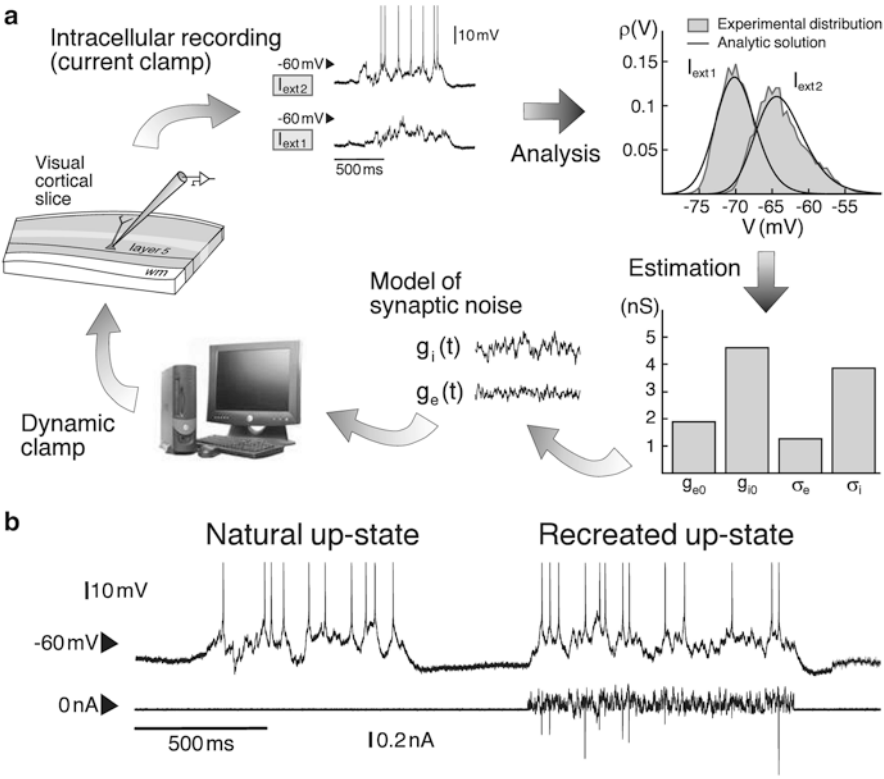

Fig. 8.7 VmD method and test using dynamic-clamp experiments. (**a**) VmD conductance estimation and test of the estimates. *Top left*: spontaneous active network states ("up-states") were recorded intracellularly in ferret visual cortex slices at two different injected current levels (I_{ext1}, I_{ext2}). *Top right*: the V_m distributions (*gray*) were computed from experimental data and used to estimate synaptic conductances using the VmD method (analytic expression of V_m distribution shown by *solid lines*). *Bottom right*: histogram of the mean and standard deviation of excitatory and inhibitory conductances obtained from the fitting procedure (*gray*). *Bottom left*: a dynamic-clamp protocol was used to inject stochastic conductances consistent with these estimates, therefore recreating artificial up-states in the same neuron. (**b**) Example of natural and recreated up-states in the same cell as in (**a**). This procedure recreated V_m activity similar to the active state. Figure modified from Rudolph et al. 2004

The match between the original V_m distribution with the one obtained synthetically demonstrated that the VmD method provides good conductance estimates.

The main advantage of the VmD method is that it provides a full characterization of the stochastic conductances. Like other "classic" methods of conductance estimation (reviewed in Monier et al. 2008), the VmD method provides estimates of the total (mean) level of excitatory and inhibitory conductances (g_{e0}, g_{i0}). In addition, it also provides estimates of the *conductance fluctuations*, through the standard deviation of conductances (σ_e, σ_i). This information is not readily obtained by other

methods but is important because it provides estimates of the respective contributions of excitation and inhibition to the V_m fluctuations, and thus offers a quantitative characterization of the "synaptic noise."

Another advantage of the VmD method is that it does not require to record in voltage-clamp mode, which considerably simplifies the experimental protocols, as everything can be estimated from recordings of the V_m activity (current-clamp). However, action potentials must be removed, because the associated Na^+ and K^+ conductances can significantly bias the VmD estimates, so the V_m distributions must be estimated exclusively by accumulating periods of subthreshold activity in-between spikes. Using such a procedure, the VmD method was applied to intracellular recordings in vivo during anesthetized states (Rudolph et al. 2005) and in awake cats (Rudolph et al. 2007). The latter provided the first quantitative conductance estimates in awake animals.

Estimating the Optimal Conductance Patterns Leading to Spikes in "Noisy" States

The estimation of conductance fluctuations by the VmD method had an important consequence: it opened the route to experimentally characterize the influence of fluctuations on action potential generation. This was the object of a recent method to estimate the spike-triggered average (STA) conductance patterns from V_m recordings (Pospischil et al. 2007). This "STA method" is also based on the point-conductance model, and requires the prior knowledge of the parameters of mean excitatory and inhibitory conductances (g_{e0}, g_{i0}) and their variances (σ_e, σ_i), which can be provided by the VmD method. Using this knowledge, one can use a maximum likelihood estimator to compute the STA conductance patterns. Similar to the VmD method, the STA method was also tested using dynamic-clamp experiments and was shown to provide accurate estimates (Pospischil et al. 2007; Piwkowska et al. 2008).

Figure 8.8 illustrates STA estimates in a computational model reproducing two extreme conditions found experimentally. First, states where both excitatory and inhibitory conductances are of relatively low and comparable amplitude ("Equal conductance," left panels in Fig. 8.8), similar to some measurements (Shu et al. 2003; Haider et al. 2006). Second, cases where the inhibitory conductance can be up to several-fold larger than the excitatory conductance ("Inhibition-dominated," right panels in Fig. 8.8), which was observed in other measurements in anesthetized (Borg-Graham et al. 1998; Hirsch et al. 1998; Destexhe et al. 2003; Rudolph et al. 2005) or awake preparations (Rudolph et al. 2007). These two extreme cases produce similar mean V_m and V_m fluctuations, but they predict different patterns of conductance STA, as shown in Fig. 8.8B. In the "Equal conductance" condition, the total conductance increases before the spike, and this increase is necessarily due to excitation. In "Inhibition-dominated" neurons, the opposite pattern is seen: there is

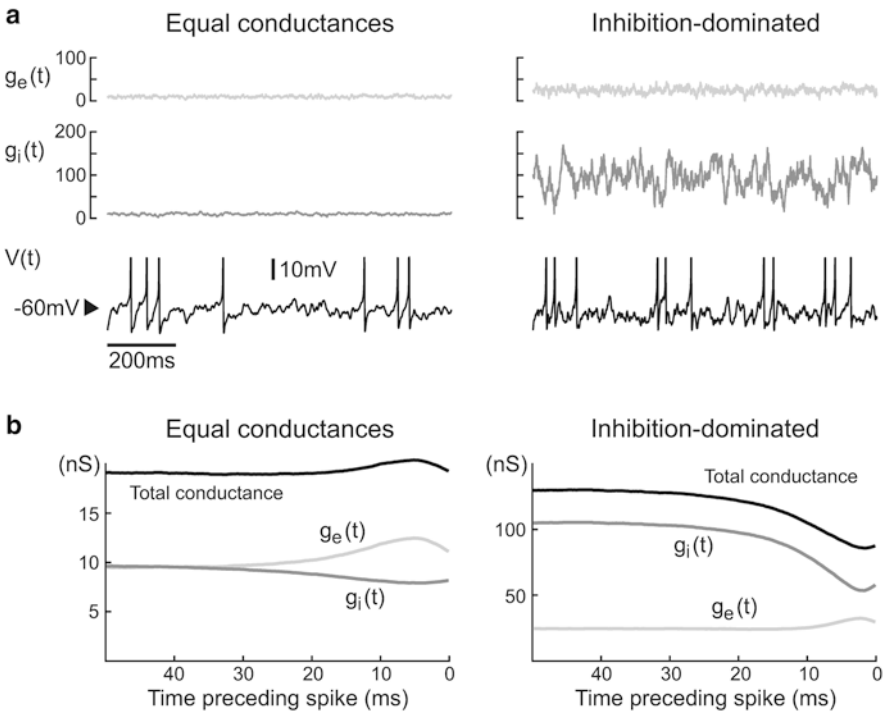

Fig. 8.8 Two patterns of conductances associated to generating spikes in model neurons. Two different "states" are displayed, both leading to comparable V_m fluctuations. *Left*: "Equal conductance" pattern, where g_e and g_i are of comparable amplitude and statistics. *Right*: "Inhibition-dominated" pattern, where g_{e0} is stronger than with equal conductances, but g_{i0} needs to be several-fold larger to maintain the V_m at a similar level. (**a**) g_e, g_i, and V_m activity. (**b**) Spike-triggered conductance patterns associated to each state. Figure modified from Rudolph et al. 2007

a decrease of total conductance prior to the spike, and this decrease necessarily comes from the decrease of inhibition before the spike.

To determine which conductance pattern is seen in cortical neurons in vivo, we applied the STA method to intracellular recordings in awake cats (Rudolph et al. 2007). From intracellular recordings of electrophysiologically identified RS cells, we evaluated the STA of excitatory and inhibitory conductances, as well as the total conductance preceding the spike for neurons recorded in awake (Fig. 8.9A, top) or naturally sleeping (Fig. 8.9A, bottom) cats (see details in Rudolph et al. 2007). In most cells tested (7 out of 10 cells in awake, 6 out of 6 cells in slow-wave sleep, and 2 out of 2 cells in REM sleep), the total conductance drops before the spike, in yielded STAs qualitatively equivalent to that of the model when inhibition is dominant (Fig. 8.8B, right panels).

Note that this pattern is opposite to what is expected from feed-forward inputs. A feed-forward drive would predict an increase of excitation closely associated to an

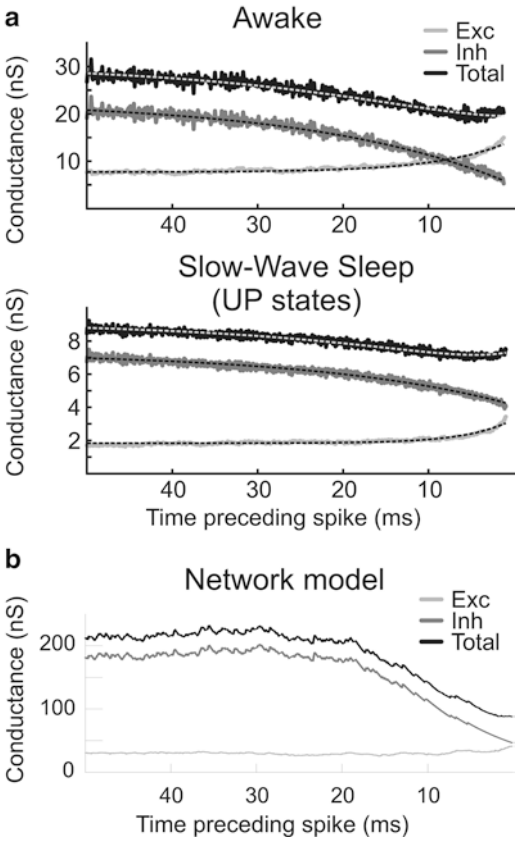

Fig. 8.9 Evidence for "Inhibition-dominated" states in wake and sleep states, as well as in network models. (**a**) Spike-triggered average (STA) of the excitatory, inhibitory, and total conductances obtained from intracellular data of regular-spiking neurons in an awake (*top*) and sleeping (slow-wave sleep up-states, *bottom*) cat. The estimated conductance time courses showed in both cases a drop of the total conductance caused by a marked drop of inhibitory conductance within about 20 ms before the spike. (**b**) STA of conductances in a representative neuron in a network model displaying self-sustained asynchronous irregular states. A 10,000-cell network of integrate-and-fire neurons with conductance-based synaptic interactions was used (see details in El Boustani et al. 2007). (**a**) Modified from Rudolph et al. 2007; (**b**) modified from El Boustani et al. 2007

increase of inhibition, as seen in many instances of evoked responses during sensory processing (Borg-Graham et al. 1998; Monier et al. 2003; Wehr and Zador 2003; Wilent and Contreras 2005). There is no way to account for a concerted g_e increase and g_i drop without invoking recurrent activity, except if the inputs evoked a strong disinhibition, but this was so far not observed in conductance measurements. Indeed, this pattern with inhibition drop was found in self-generated irregular states in networks of integrate-and-fire neurons (Fig. 8.9B; see details in El Boustani et al. 2007). This constitutes direct evidence that most spikes in neocortex in vivo are caused by recurrent (internal) activity, and not by evoked (external) inputs.

Discussion

In this chapter, we have overviewed several recent developments of the exploration of the integrative properties of central neurons in the presence of "noise." This theme has been popular in modeling studies, starting from seminal work (Barrett and Crill 1974; Barrett 1975; Bryant and Segundo 1976; Holmes and Woody 1989), which was followed by compartmental model studies (Bernander et al. 1991; Rapp et al. 1992; De Schutter and Bower 1994). In the last 2 decades, significant progress was made in several aspects of this problem.

The first aspect which we overviewed here is that background activity was measured quantitatively for the first time in "activated" network states in vivo (Paré et al. 1998). Based on these quantitative measurements, constrained models could be built (Destexhe and Paré 1999) to investigate integrative properties in realistic in vivo-like activity states. Consequences on dendritic integration, such as coincidence detection and enhanced temporal processing, as predicted (Bernander et al. 1991; Softky 1994), were confirmed (Rudolph and Destexhe 2003b). New consequences were also found, such as enhanced responsiveness (Hô and Destexhe 2000) and location-independent synaptic efficacy (Rudolph and Destexhe 2003b). The first of these predictions was confirmed by dynamic-clamp experiments (Destexhe et al. 2001; Chance et al. 2002; Fellous et al. 2003; Mitchell and Silver 2003; Prescott and De Koninck 2003; Shu et al. 2003; Higgs et al. 2006).

We reviewed another aspect that tremendously progressed, namely the formulation of simplified models that replicate the in vivo measurements, as well as important properties such as the typical Lorentzian spectral structure of background activity. This point-conductance model (Destexhe et al. 2001) had many practical consequences, such as to enable dynamic-clamp. Indeed, many of the aforementioned dynamic-clamp studies used the point-conductance model to recreate in vivo-like activity states in neurons maintained in vitro. In addition to confirm model predictions, dynamic-clamp experiments also took these concepts further and investigated important properties such as gain modulation (Chance et al. 2002; Fellous et al. 2003; Mitchell and Silver 2003; Prescott and De Koninck 2003). An inverse form of gain modulation can also be observed (Fellous et al. 2003) and may be explained by potassium conductances (Higgs et al. 2006). It was also found that the intrinsic properties of neurons combine with synaptic noise to yield unique responsiveness properties (Wolfart et al. 2005).

It must be noted that although the point-conductance model was the first model of fluctuating synaptic conductances injected in living neurons using dynamic-clamp, other models are also possible. For example, models based on the convolution of Poisson processes with exponential synaptic waveforms ("shot noise") have also been used (e.g., see Chance et al. 2002; Prescott and De Koninck 2003). However, it can be shown that these models are in fact equivalent, as the point-conductance model can be obtained as a limit case of a shot-noise process with exponential conductances (Destexhe and Rudolph 2004).

An important consequence, specific to the point-conductance model, is that its mathematical simplicity enabled formulation of a number of variants of the Fokker–Planck

equation for the membrane potential probability density (Rudolph and Destexhe 2003a, 2005; Richardson 2004; Lindner and Longtin 2006), which led to a method to estimate synaptic conductances from V_m recordings (Rudolph et al. 2004). This "VmD method" decomposed the V_m fluctuations into excitatory and inhibitory contributions, estimating their mean and variance. This method was successfully tested in dynamic-clamp experiments (Rudolph et al. 2004) as well as in voltage-clamp (Greenhill and Jones 2007; see also Ho et al. 2009). The most interesting aspect of the VmD method is that it provides estimates of the variance of conductances or, equivalently, conductance fluctuations. This type of estimate was made for cortical neurons during artificially activated brain states (Rudolph et al. 2005) or in awake animals (Rudolph et al. 2007). The latter provided the first quantitative characterization of synaptic conductances and their fluctuations in aroused animals.

Finally, this approach was extended to estimate dynamic properties related to action potential initiation. If the information about synaptic conductances and their fluctuations is available (for example following VmD estimates), then one can use maximum likelihood methods to evaluate the spike-triggered conductance patterns. This information is very important to determine which optimal conductance variations determine the "output" of the neuron, which is a fundamental aspect of integrative properties. We found that in awake and naturally sleeping animals, the majority of spikes are statistically related to disinhibition, which plays a permissive role. This type of conductance dynamics is opposite to the conductance patterns evoked by external input, but can be replicated by models displaying self-generated activity. This suggests that most spikes in awake animals are due to internal network activity. This argues for a dominant role of the network state in vivo and that inhibition is a key player. Both aspects should be investigated by future studies.

Thus, the last 20 years have seen a tremendous theoretical and experimental characterization of the synaptic "noise," and its consequences on neurons and networks. Computational models have played—and still continue to play—a pivotal role in this exploration.

Acknowledgments The experimental data shown here were obtained in collaboration with Thierry Bal, Diego Contreras, Jean-Marc Fellous, Denis Paré, Zuzanna Piwkowska, Mircea Steriade and Igor Timofeev. The models and analyses were done in collaboration with Sami El Boustani, Martin Pospischil, Michelle Rudolph and Terrence Sejnowski. Research supported by the CNRS, ANR (HR-CORTEX project), HFSP and the European Community (FACETS project FP6-15879; BrainScales project FP7-269921).

References

Barrett JN (1975) Motoneuron dendrites: role in synaptic integration. Fed Proc 34:1398–1407

Barrett JN, Crill WE (1974) Influence of dendritic location and membrane properties on the effectiveness of synapses on cat motoneurones. J Physiol 293:325–345

Bernander O, Douglas RJ, Martin KA, Koch C (1991) Synaptic background activity influences spatiotemporal integration in single pyramidal cells. Proc Natl Acad Sci USA 88:11569–11573

Borg-Graham LJ, Monier C, Frégnac Y (1998) Visual input evokes transient and strong shunting inhibition in visual cortical neurons. Nature 393:369–373
Bryant HL, Segundo JP (1976) Spike initiation by transmembrane current: a white-noise analysis. J Physiol 260:279–314
Chance FS, Abbott LF, Reyes AD (2002) Gain modulation from background synaptic input. Neuron 35:773–782
Contreras D, Timofeev I, Steriade M (1996) Mechanisms of long lasting hyperpolarizations underlying slow sleep oscillations in cat corticothalamic networks. J Physiol 494:251–264
De Schutter E, Bower JM (1994) Simulated responses of cerebellar Purkinje cells are independent of the dendritic location of granule cell synaptic inputs. Proc Natl Acad Sci USA 91:4736–4740
Destexhe A (2007) High-conductance state. Scholarpedia 2:1341. http://www.scholarpedia.org/article/High-Conductance State
Destexhe A, Bal T (eds) (2009) The dynamic-clamp: from principles to applications. Springer, New York
Destexhe A, Paré D (1999) Impact of network activity on the integrative properties of neocortical pyramidal neurons in vivo. J Neurophysiol 81:1531–1547
Destexhe A, Rudolph M (2004) Extracting information from the power spectrum of synaptic noise. J Comput Neurosci 17:327–345
Destexhe A, Rudolph M (2012) Neuronal noise. Springer, New York
Destexhe A, Contreras D, Steriade M (1999) Spatiotemporal analysis of local field potentials and unit discharges in cat cerebral cortex during natural wake and sleep states. J Neurosci 19:4595–4608
Destexhe A, Rudolph M, Fellous J-M, Sejnowski TJ (2001) Fluctuating synaptic conductances recreate in vivo-like activity in neocortical neurons. Neuroscience 107:13–24
Destexhe A, Mand R, Paré D (2003) The high-conductance state of neocortical neurons *in vivo*. Nat Rev Neurosci 4:739–751
El Boustani S, Pospischil M, Rudolph-Lilith Mand Destexhe A (2007) Activated cortical states: experiments, analyses and models. J Physiol Paris 101:99–109
Fellous JM, Rudolph M, Destexhe A, Sejnowski TJ (2003) Synaptic background noise controls the input/output characteristics of single cells in an in vitro model of in vivo activity. Neuroscience 122:811–829
Gammaitoni L, Hanggi P, Jung P, Marchesoni F (1998) Stochastic resonance. Rev Mod Phys 70:223–287
Greenhill SD, Jones RS (2007) Simultaneous estimation of global background synaptic inhibition and excitation from membrane potential fluctuations in layer III neurons of the rat entorhinal cortex in vitro. Neuroscience 147:884–892
Haider B, McCormick DA (2009) Rapid neocortical dynamics: cellular and network mechanisms. Neuron 62:171–189
Haider B, Duque A, Hasenstaub AR, McCormick DA (2006) Neocortical network activity in vivo is generated through a dynamic balance of excitation and inhibition. J Neurosci 26: 4535–4545
Higgs MH, Slee SJ, Spain WJ (2006) Diversity of gain modulation by noise in neocortical neurons: regulation by the slow after-hyperpolarization conductance. J Neurosci 26:8787–8799
Hirsch JA, Alonso JM, Reid RC, Martinez LM (1998) Synaptic integration in striate cortical simple cells. J Neurosci 18:9517–9528
Hô N, Destexhe A (2000) Synaptic background activity enhances the responsiveness of neocortical pyramidal neurons. J Neurophysiol 84:1488–1496
Ho EC, Zhang L, Skinner FK (2009) Inhibition dominates in shaping spontaneous CA3 hippocampal network activities in vitro. Hippocampus 19:152–165
Holmes WR, Woody CD (1989) Effects of uniform and non-uniform synaptic "activation-distributions" on the cable properties of modeled cortical pyramidal neurons. Brain Res 505:12–22
Lindner B, Longtin A (2006) Comment on "Characterization of subthreshold voltage fluctuations in neuronal membranes", by M. Rudolph and A. Destexhe. Neural Comput 18:1896–1931

Llinas RR, Jahnsen H (1982) Electrophysiology of thalamic neurones in vitro. Nature 297:406–408
Mitchell SJ, Silver RA (2003) Shunting inhibition modulates neuronal gain during synaptic excitation. Neuron 38:433–445
Monier C, Chavane F, Baudot P, Graham LJ, Frégnac Y (2003) Orientation and direction selectivity of synaptic inputs in visual cortical neurons: a diversity of combinations produces spike tuning. Neuron 37:663–680
Monier C, Fournier J, Frégnac Y (2008) In vitro and in vivo measures of evoked excitatory and inhibitory conductance dynamics in sensory cortices. J Neurosci Methods 169:323–365
Paré D, Shink E, Gaudreau H, Destexhe A, Lang EJ (1998) Impact of spontaneous synaptic activity on the resting properties of cat neocortical neurons in vivo. J Neurophysiol 79: 1450–1460
Piwkowska Z, Pospischil M, Brette R, Sliwa J, Rudolph-Lilith M, Bal T, Destexhe A (2008) Characterizing synaptic conductance fluctuations in cortical neurons and their influence on spike generation. J Neurosci Methods 169:302–322
Pospischil M, Piwkowska Z, Rudolph M, Bal T, Destexhe A (2007) Calculating event-triggered average synaptic conductances from the membrane potential. J Neurophysiol 97:2544–2552
Prescott SA, De Koninck Y (2003) Gain control of firing rate by shunting inhibition: roles of synaptic noise and dendritic saturation. Proc Natl Acad Sci USA 100:2076–2081
Rapp M, Yarom Y, Segev I (1992) The impact of parallel fiber background activity on the cable properties of cerebellar Purkinje cells. Neural Comput 4:518–533
Richardson MJ (2004) Effects of synaptic conductance on the voltage distribution and firing rate of spiking neurons. Phys Rev E 69:051918
Risken H (1984) The Fokker Planck equation: methods of solution and application. Springer, Berlin
Robinson HP, Kawai N (1993) Injection of digitally synthesized synaptic conductance transients to measure the integrative properties of neurons. J Neurosci Methods 49:157–165
Rudolph M, Destexhe A (2001) Correlation detection and resonance in neural systems with distributed noise sources. Phys Rev Lett 86:3662–3665
Rudolph M, Destexhe A (2003a) Characterization of subthreshold voltage fluctuations in neuronal membranes. Neural Comput 15:2577–2618
Rudolph M, Destexhe A (2003b) A fast-conducting, stochastic integrative mode for neocortical dendrites *in vivo*. J Neurosci 23:2466–2476
Rudolph M, Destexhe A (2005) An extended analytic expression for the membrane potential distribution of conductance-based synaptic noise. Neural Comput 17:2301–2315
Rudolph M, Destexhe A (2006) On the use of analytic expressions for the voltage distribution to analyze intracellular recordings. Neural Comput 18:917–922
Rudolph M, Piwkowska Z, Badoual M, Bal T, Destexhe A (2004) A method to estimate synaptic conductances from membrane potential fluctuations. J Neurophysiol 91:2884–2896
Rudolph M, Pelletier J-G, Paré D, Destexhe A (2005) Characterization of synaptic conductances and integrative properties during electrically-induced EEG-activated states in neocortical neurons in vivo. J Neurophysiol 94:2805–2821
Rudolph M, Pospischil M, Timofeev I, Destexhe A (2007) Inhibition determines membrane potential dynamics and controls action potential generation in awake and sleeping cat cortex. J Neurosci 27:5280–5290
Sharp AA, O'Neil MB, Abbott LF, Marder E (1993) The dynamic clamp: artificial conductances in biological neurons. Trends Neurosci 16:389–394
Shu Y, Hasenstaub A, Badoual M, Bal T, McCormick DA (2003) Barrages of synaptic activity control the gain and sensitivity of cortical neurons. J Neurosci 23:10388–10401
Softky W (1994) Sub-millisecond coincidence detection in active dendritic trees. Neuroscience 58:13–41
Steriade M (2003) Neuronal substrates of sleep and epilepsy. Cambridge University Press, Cambridge, UK

Steriade M, Timofeev I, Grenier F (2001) Natural waking and sleep states: a view from inside neocortical neurons. J Neurophysiol 85:1969–1985
Tuckwell HC (1988) Introduction to theoretical neurobiology. Cambridge University Press, Cambridge, UK
Wehr M, Zador AM (2003) Balanced inhibition underlies tuning and sharpens spike timing in auditory cortex. Nature 426:442–446
Wiesenfeld K, Moss F (1995) Stochastic resonance and the benefits of noise: from ice ages to crayfish and SQUIDs. Nature 373:33–36
Wilent W, Contreras D (2005) Dynamics of excitation and inhibition underlying stimulus selectivity in rat somatosensory cortex. Nat Neurosci 8:1364–1370
Wolfart J, Debay D, Le Masson G, Destexhe A, Bal T (2005) Synaptic background activity controls spike transfer from thalamus to cortex. Nat Neurosci 8:1760–1767